Growth of a Bose-Einstein condensate: A detailed comparison of theory and experiment

M J Davis†‡ and C W Gardiner§

† Clarendon Laboratory, Department of Physics, University of Oxford, Parks Rd, Oxford, OX1 3PU, United Kingdom

‡ Department of Physics, University of Queensland, St Lucia, QLD 4072, Australia

§ School of Chemical and Physical Sciences, Victoria University of Wellington, Wellington, New Zealand

E-mail: m.davis2@physics.ox.ac.uk

Abstract.

We extend the earlier model of condensate growth of Davis *et al* [Davis MJ, Gardiner CW and Ballagh RJ 2000 *Phys. Rev.* A **62** 063608] to include the effect of gravity in a magnetic trap. We carry out calculations to model the experiment reported by Köhl *et al* [Köhl M, Davis MJ, Gardiner CW, Hänsch T and Esslinger T, *Preprint* cond-mat/0106642] who study the formation of a rubidium Bose-Einstein condensate for a range of evaporative cooling parameters. We find that in the regime where our model is valid, the theoretical curves agree with all the experimental data with no fitting parameters. However, for the slowest cooling of the gas the theoretical curve deviates significantly from the experimental curves. It is possible that this discrepancy may be related to the formation of a quasicondensate.

1. Introduction

The process by which a Bose-Einstein condensate (BEC) forms from a non-equilibrium thermal vapour is an important question in finite temperature field theory. Before the first observations of condensates [1, 2, 3], estimates for the characteristic time of formation varied dramatically (eg see discussion in [4]). However, more recently the quantum kinetic theory of Gardiner and Zoller [5] has resulted in quantitative predictions that can be compared with experimental data.

Until recently the only experimental study of the process of condensate formation was that performed by Miesner *et al* [6] in the group of Ketterle at MIT. In these experiments a cloud of sodium atoms was cooled to just above the BEC transition temperature, before the high-energy tail of the distribution was quickly removed by a rapid sweep of the rf field frequency. The resulting dynamics lead to the formation of a condensate, with the observation of characteristic S-shaped growth curves.

Before the first measurements of condensate growth, a quantitative prediction of the growth rate was presented in [7], in which a condensate was assumed to form

from contact with a thermal bath below the transition temperature. In order to give a simple estimate of the rate constant, the approach was greatly simplified and had several limitations—the most important being the use of a Maxwell-Boltzmann rather than Bose-Einstein distribution function for the thermal bath. However, it gave a good qualitative prediction of the general shape and order of magnitude of the growth rate later observed.

This model was soon extended to include both Bose-Einstein statistics for the thermal bath of atoms, and the dynamics of the lowest lying quasiparticle levels above the condensate [8, 9]. The picture was of a condensate band in contact with a "supersaturated" thermal cloud, and the assumptions of the model matched the experimental conditions realized at MIT quite closely. A comparison of the theoretical predictions with experimental data was in good agreement at higher temperatures; however, at lower temperatures there was some discrepancy—the experimental growth rate appeared to be about three times too fast.

In further development, this model was again extended to include the dynamics of the evaporative cooling in [10]. While this predicted faster growth in some circumstances as compared to the simpler model, it did not occur in the parameter regime of the MIT experiment and thus the discrepancy remained. In addition, the necessary experimental data for a proper theoretical treatment was not available. It was concluded that for a rigorous comparison with theory it was necessary for further experiments to be carried out with all relevant data recorded. The same conclusion was reached in a similar calculation by Bijlsma *et al* [11].

Recently a carefully controlled study of condensate formation in a rubidium vapour was carried out by Köhl *et al* [12] in Munich. They used a different cooling scheme from that used in the the MIT experiment—instead of a rapid rf sweep after cooling to near the transition temperature, they turned on a constant frequency rf field. This allowed them to vary the rate of evaporative cooling by changing the rf frequency between experiments, and they report their growth curves, initiation times, and growth rates in [12]. Most importantly, the Munich group measured all the relevant theoretical parameters, so that calculations with *no free parameters* can be carried out.

This paper is organized as follows. In section 2 we summarize the theoretical model of [10], before describing the extensions necessary to model the experiments of Köhl *et al* [12] and discussing the validity of the approximations made. In section 3 we investigate the effect of the model extensions on condensate growth as compared to the earlier calculations in [10], and then compare the results of the model to the experimental data and discuss their implications. Finally, our conclusions are presented in section 4.

2. Theoretical model

The model we use to simulate the experiments of Köhl *et al* is described fully in reference [10]. The description is based on quantum kinetic theory [5], but essentially reduces to solving a modified ergodic quantum Boltzmann equation (MQBE) that assumes

the distribution function depends only on energy. Our method makes the additional assumptions that:

(i) The condensate wave function and energy eigenvalue [the condensate chemical potential $\mu_{\rm C}(n_0)$] are given by the solution of the time-independent Gross-Pitaevskii equation with n_0 atoms. We assume that the growth of the condensate is adiabatic and that its shape is always well-described by the Thomas-Fermi wave function.

(ii) The excited states above the condensate are the quasiparticle levels appropriate to the condensate wave function, leading to a density of states for the system that is substantially modified from the non-interacting case. We use a particle-like density of states, thus neglecting any specifically quasiparticle behaviour, whose effects are expected to be minor [13].

To model the MIT experiments, the simulations were begun with an initial distribution truncated at an energy $\epsilon_{\rm cut}$ and so the process of atom loss during the evaporative cooling did not need to be included. However, as the Munich experiment involves continuous evaporative cooling, it must be included in the simulation. To do so we solve the effective MQBE

$$g_n \frac{\partial f_n}{\partial t} = \frac{8ma^2}{\pi\hbar^3} \sum_{pqm} g_{\rm min}\delta(\epsilon_p + \epsilon_q - \epsilon_m - \epsilon_n) \times \{\beta_n f_p f_q (1+f_m)(1+f_n) - f_m f_n (1+f_q)(1+f_q)\} \quad (1)$$

where a is the s-wave scattering length, m is the atomic mass, $f_n \equiv f(\epsilon_n)$ is the distribution function, $g_n \equiv g(\epsilon_n)$ is the density of states, and $g_{\rm min}$ is the density of states of the minimum energy particle participating in the collision. The quantity β_n takes account of the evaporative cooling—it is one if the energy $\epsilon_n \geq \epsilon_{\rm cut}$, and zero otherwise.

There is, however, another effect that must be taken account of at low temperatures. The trapping potential that the atoms experience is due to not only the applied magnetic field, but also the gravitational potential. While gravity does not change the shape of the trapping potential, it shifts the minimum of the trap away from the minimum of the magnetic field. This has important consequences for the evaporative cooling of the cloud. Before we describe this further, however, we summarize the initial parameters of the experiment we are modelling so we can quantitatively discuss the magnitude of the effect.

2.1. Experimental summary

The magnetic trap used by Köhl *et al* is well approximated by a cigar-shaped harmonic potential with trapping frequencies $\omega_x = \omega_z = 2\pi \times 110$ Hz, $\omega_y = 14$ Hz, with a geometric mean frequency of $\bar{\omega} = (\omega_x\omega_y\omega_z)^{1/3} = 2\pi \times 55.3$ Hz. They begin their growth experiments with a cloud of $N_i = 4.2 \pm 0.2 \times 10^6$ atoms of ^{87}Rb trapped in the $|F = 1, m_F = -1\rangle$ hyperfine ground state, cooled to a temperature of 640 ± 30 nK giving an initial chemical potential of $\mu_{\rm init} \approx -300\hbar\bar{\omega}$. The rf fields they applied to

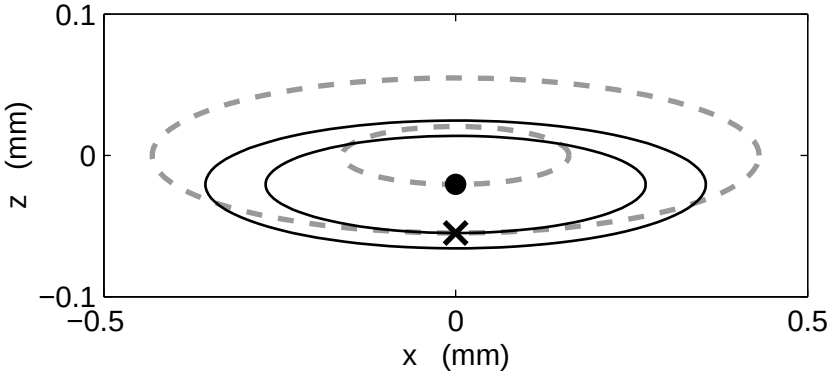

Figure 1. An indication of the sag of the trapping potential as compared to the magnetic field equipotentials. The dashed gray lines indicate the magnetic equipotentials corresponding to an rf field frequency of 1955 kHz (inner) and 2090 kHz (outer). The solid dot indicates the centre of the atomic cloud. The solid lines represent the spatial bounds of atoms with an energy of $4.62k_BT_i$ (inner) and $8k_BT_i$ (outer). The cross marks the innermost intersection of the rf field with atomic cloud equipotentials, determining the quantity $\eta = 4.62$. However, as can be seen there can be atoms with energy $8k_BT_i$ in orbits that will not be ejected from the trap via spin flips.

their cloud for which a condensate was observed to form were between 2000–2090 kHz, corresponding to $0.92 \leq \eta \equiv \epsilon_{\rm cut}/k_BT_i \leq 4.62$.

2.2. Gravitational sag of the trapped atomic cloud

By including the effect of gravity, we find that the trapping potential the atoms experience is given by

$$V(\mathbf{r}) = \frac{m}{2}\left[\omega_x^2 x^2 + \omega_y^2 y^2 + \omega_z^2 (z + A)^2\right] \tag{2}$$

where the origin is defined as the minimum of the magnetic field, and $A = g/\omega_z^2 = 20.5$ μm is the sag of the atom cloud below the origin. This situation is illustrated in figure 1.

The sag of the atomic cloud has important consequences for evaporative cooling at low temperatures. In figure 1 the solid dot represents the centre of the atomic cloud, while the dashed grey curves represent magnetic field equipotentials. The innermost corresponds to an rf field frequency of 1955kHz, which was determined to be the minimum of the trap by atom laser output coupling [12]. The outermost dashed grey curve represents an rf field frequency of 2090 kHz applied to the system, and all atoms that cross this surface will be quickly ejected from the trap.

By considering the intersection of the equipotentials of the atomic cloud with the evaporative cooling surface, we find that all atoms with an energy less than $\epsilon_{\rm cut} = 4.62k_BT_i$ will remain trapped. However, not all atoms with higher energy will be ejected—as can be seen by considering the equipotential corresponding to $\epsilon = 8k_BT_i$. Atoms with this energy in a horizontal orbit will not cross the evaporative cooling surface, and hence will remain trapped at least until they suffer another collision.

2.2.1. Inclusion of sag in model One of the limitations of our theoretical model is that the distribution function of the gas is assumed to be ergodic—that is, all states of the gas with the same energy are assumed to have the same occupation. This obviously cannot hold rigorously in this situation, where atoms of the same energy will be ejected depending on orientation of their orbit. However, the effect of the sag of the cloud can be included in the model, if not entirely rigorously.

We proceed to calculate the fraction of atoms of a given energy that will remain trapped during the application of a fixed frequency rf field, and use this as our function $\beta(\epsilon_n)$ in equation (1). As the hottest atoms are ejected from the trap it is reasonable to assume that they can be treated as being non-interacting. Indeed, we found in reference [10] that the density of states we use is not greatly altered from the non-interacting case for energies larger than about three times the condensate eigenvalue, which in these calculations never exceeds $45\hbar\bar{\omega}$. In comparison the minimum energy for ejection is about $k_B T_i \approx 240\hbar\bar{\omega}$ so this approximation does seem reasonable.

While it is possible to write down an integral describing the total number of states of a given energy in phase space that will remain trapped, it is not possible to to give an analytic expression for this quantity. Instead we proceed using a Monte Carlo simulation of non-interacting particles in the trap. For each energy we populate the initial states at random and then follow the trajectories in time, removing each that crosses the evaporative cooling surface. After a sufficiently long period we determine the proportion that remain trapped.

The curves we have calculated are illustrated in figure 2 as a function of the applied frequency of the rf field. For comparison we also plot the initial distribution function of the cloud. We can see that for all applied fields the region where a finite fraction of atoms is trapped is quite wide, and therefore this effect is important for the experiment we are considering here.

2.2.2. Validity of the model of the sag The inclusion of the function $\beta(\epsilon_n)$ in equation (1) relies on two approximations. The first is that an atom gaining an energy higher than $\epsilon_{\rm cut}$ is equally likely to enter any region of phase space available to it. This should be reasonable, as most collisions that result in one particle entering this region will occur between two atoms with energies less than $\epsilon_{\rm cut}$, where the distribution function should be ergodic. The second assumption is that non-ergodicity of the levels above $\epsilon_{\rm cut}$ will not have a significant effect on the calculation. This remains unproven—however, it could be tested via Monte Carlo simulations of evaporative cooling well above the BEC transition.

2.3. Other effects

A further measurement reported by Köhl *et al* is a drift in the magnetic field due to heating in the coils in the experiment, equivalent to a linear decrease in the rf field frequency of 5 kHz s^{-1}. This is easily included in our model by making the function

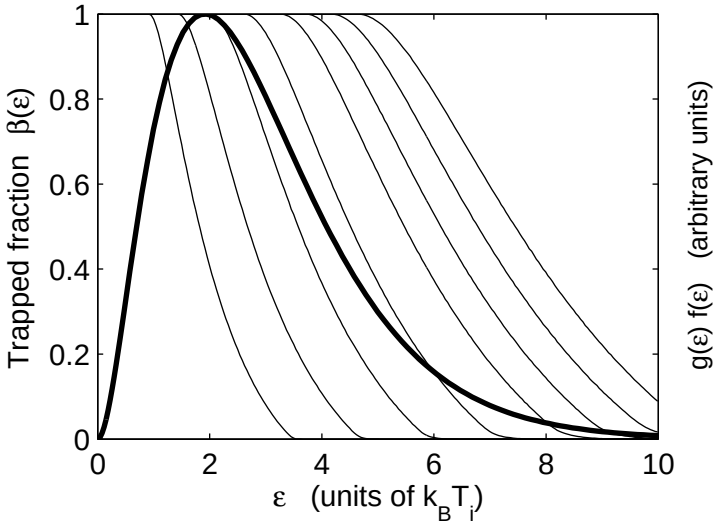

Figure 2. Curves showing the fraction of trapped atoms for a given energy with the application of rf fields: from left to right $\nu = 2000$, 2015, 2030, 2045, 2060, 2070, 2080, 2090 kHz. The solid black line is a plot of the initial distribution function of the gas $g(\epsilon)f(\epsilon)$ at $T_i = 640$ nK.

$\beta(\epsilon_n)$ time dependent.

Another factor that we include in our simulations is the loss of condensate atoms due to three body processes, via the rate

$$\frac{dn_0}{dt} = -K_3 \int d^3\mathbf{x}[n(\mathbf{x})]^3, \tag{3}$$

where $n(\mathbf{x})$ is the condensate density, and K_3 is the three body loss coefficient. Using the Thomas-Fermi profile for the condensate density we find [14]

$$\frac{dn_0}{dt} = -K_3 \frac{15^{4/5}}{168\pi^2} \left(\frac{m\bar{\omega}}{\hbar\sqrt{a}}\right)^{12/5} n_0^{9/5}, \tag{4}$$

where loss processes involving thermal cloud atoms have been neglected. This should be a reasonable approximation, as although such losses are enhanced by a factor of 3!, the density of the thermal cloud is significantly less than that of the condensate. We use a value of $K_3 = 5.8 \times 10^{-30}$ cm^6 s^{-1} for the hyperfine state $|F = 1, m_F = -1\rangle$ as reported by JILA [15].

3. Results

In this section we begin our simulations with the initial conditions as reported by Köhl *et al* and summarized in section 2.1, and use a scattering length for ^{87}Rb of $a = 110a_0$. Note that this value is subject to an uncertainty of a few percent and this could have a effect on the results, mainly through a scaling of the time axis.

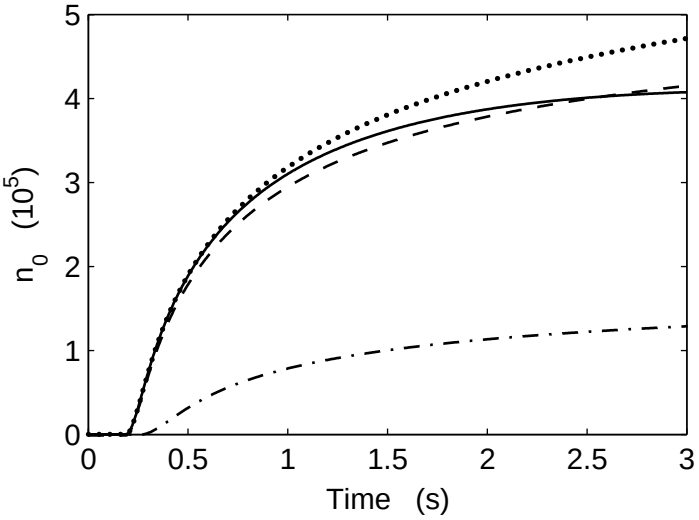

Figure 3. Growth curves from an initial condition of $N_i = 4.2 \times 10^6, T_i = 640$ nK, $\mu_{\rm init} = -300\hbar\bar{\omega}$, with an applied rf field of 2015kHz. The dot-dash line indicates the predicted condensate formation if all atoms above an energy of $\epsilon_{\rm cut}/(k_B T_i) = 1.43$ are removed from the trap. The dashed line takes into account the trap sag, and proportion of atoms lost at each energy is displayed in figure 2. The dotted line also includes the effect of the drift of the magnetic field, and finally the solid line additionally includes three body loss from the condensate.

3.1. Consequences of the trap sag and magnetic field drift

The offset of the atomic trap from the mininum of the magnetic field has a significant quantitative effect on the resulting growth curves, and this is illustrated in figure 3 for the initial condition $N_i = 4.2 \times 10^6$, $T_i = 640$ nK and an applied rf field of 2015 kHz. This gives a minimum energy of atoms to be lost from the trap of $\epsilon_{\rm cut}/(k_B T_i) = 1.43$ at $t = 0$ s.

If *all* atoms above the energy $\epsilon_{\rm cut}$ are continuously removed from the trap (dot-dash curve) [as if both the trap and magnetic field equipotentials were concentric], then the resulting condensate is much smaller than is predicted if we include the effects of the trap sag (dashed line). This is because such a heavy cut into the cloud removes a large proportion of the initial number of atoms; however, the final condensate fractions for both curves are similar. The further inclusion of the magnetic field drift (dotted line) has only the effect of making the final condensate slightly larger—easily understood as this evaporatively cools the cloud further. Finally, including three body loss from the condensate makes the growth curve start to level off once $n_0 \approx 3 \times 10^5$. The same qualitative behaviour is observed for all values of the rf field.

If a similar experiment to those carried out by Miesner *et al* [6] at MIT was performed with this initial condition—all atoms above $\epsilon_{\rm cut}/(k_B T_i) = 1.43$ are removed but with the rf field turned off at $t = 0$ s—then no condensate is observed to form. This is because the initial cloud is sufficiently far from the transition point that this single truncation cools the cloud from $\mu_{\rm init} = -300\hbar\bar{\omega}$ to $\mu_{\rm init} \approx 0$, just before condensation

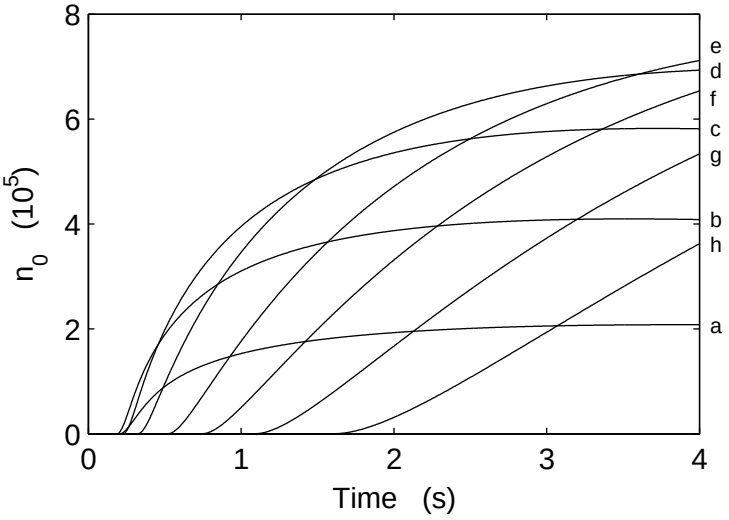

Figure 4. Growth curves from an initial condition of $N_i = 4.2 \times 10^6, T_i = 640$ nK, $\mu_{\rm init} = -300\hbar\bar{\omega}$, for rf fields of (a) 2000, (b) 2015, (c) 2030, (d) 2045, (e) 2060, (f) 2070, (g) 2080, (h) 2090 kHz.

occurs.

3.2. Trends in the theoretical data

We now present the theoretical predictions for all experimental rf frequencies in figure 4, including the effects of all of: Trap sag, magnetic field drift, and three body loss from the condensate. We show these on the same figure for comparison of time scales—in the comparison with experimental data below we show only single curves on each graph.

These curves show the expected behaviour—the fastest evaporative cooling generally results in a shorter initiation time and more rapid initial growth. However, because the fastest evaporative cooling initially loses a large number of atoms without any collisions (the cloud is simply truncated, rather than collisions causing atoms to be evaporated), this results in smaller condensates. This is the behaviour that was observed in the MIT-style simulations performed in [11].

3.3. Comparison with experimental data

In this section we compare the results of our simulations as described above with the experimental data provided by the Munich group. In figures 5 and 6 we show the condensate growth data for all experimental runs, along with four corresponding theoretical curves for each run. The solid lines are for the initial conditions reported by Köhl *et al*, and the others are within the statistical error with a chemical potential slightly closer to zero (ie lower temperatures and larger number of atoms). Thus we do not present curves within the statistical error that begin *further* from the transition than the central value. We do not include background loss in the simulations as the trap lifetime was more than 40 seconds [16].

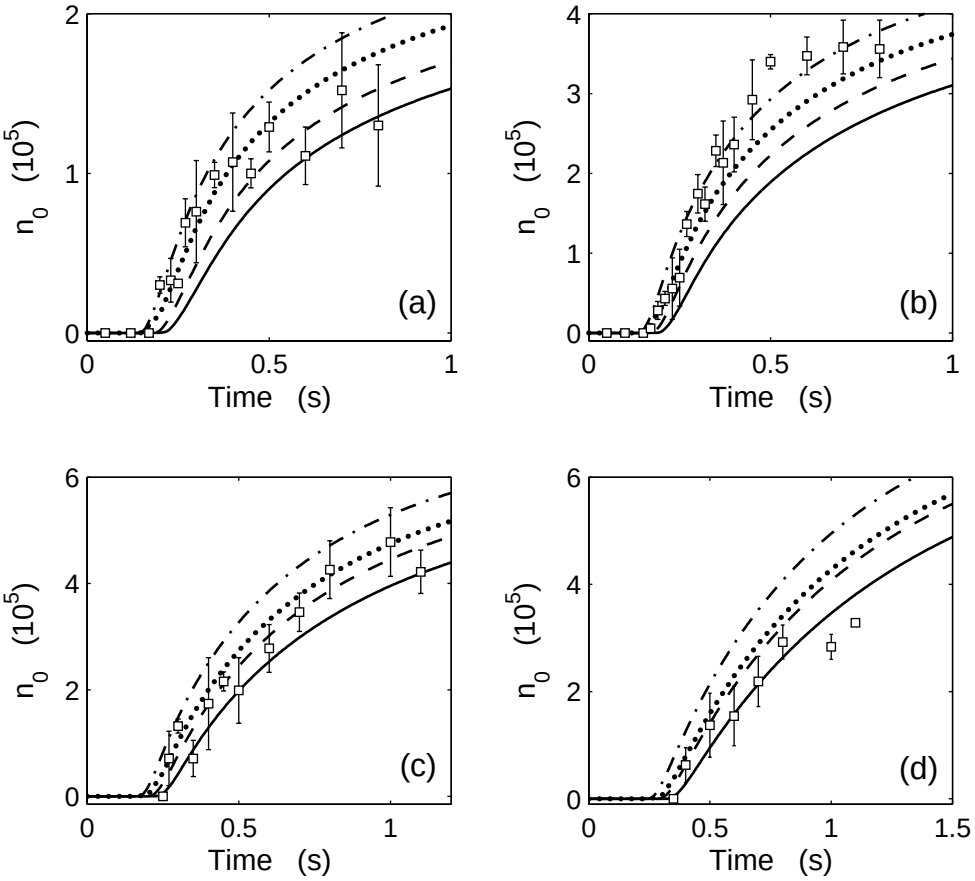

Figure 5. Comparison of theory and experiment for the growth of a ^{87}Rb Bose-Einstein condensate. The squares with error bars indicate the experimental data, while each line is the theoretical prediction based on a slightly different initial condition. Each graph is for a different rf frequency ν. Solid: $N_i = 4.2 \times 10^6$, $T_i = 640$ nK, $\mu_{\rm init} = -300\hbar\bar{\omega}$. Dashed: $N_i = 4.4 \times 10^6$, $T_i = 640$ nK, $\mu_{\rm init} = -289\hbar\bar{\omega}$. Dotted: $N_i = 4.2 \times 10^6$, $T_i = 610$ nK, $\mu_{\rm init} = -254\hbar\bar{\omega}$. Dot-dash: $N_i = 4.4 \times 10^6$, $T_i = 610$ nK, $\mu_{\rm init} = -244\hbar\bar{\omega}$. (a) $\nu = 2000$ kHz. (b) $\nu = 2015$ kHz. (c) $\nu = 2030$ kHz. (d) $\nu = 2045$ kHz.

Considering the fact that there are *no free parameters* in these calculations, the fits of the theoretical curves to the experimental data are impressive. For the rf frequencies 2000–80 kHz the initiation times for condensate growth are predicted extremely well, along with the initial rates of condensate growth. It does seem for the slower growth curves with rf frequencies 2060–80 kHz that the condensate occupation curve levels off somewhat faster than the model predicts. Unfortunately there is no experimental data at later times to determine whether the condensate continues to grow.

The cause of the flattening of these growth curves for these rf frequencies is as yet undetermined. It was originally suggested that there could be a small amount of heating present in the system that only becomes apparent in the longer experiments. However, careful analysis of the experimental data [16] has ruled out this mechanism as an explanation for the slow down of condensate growth. A second possibility is that the

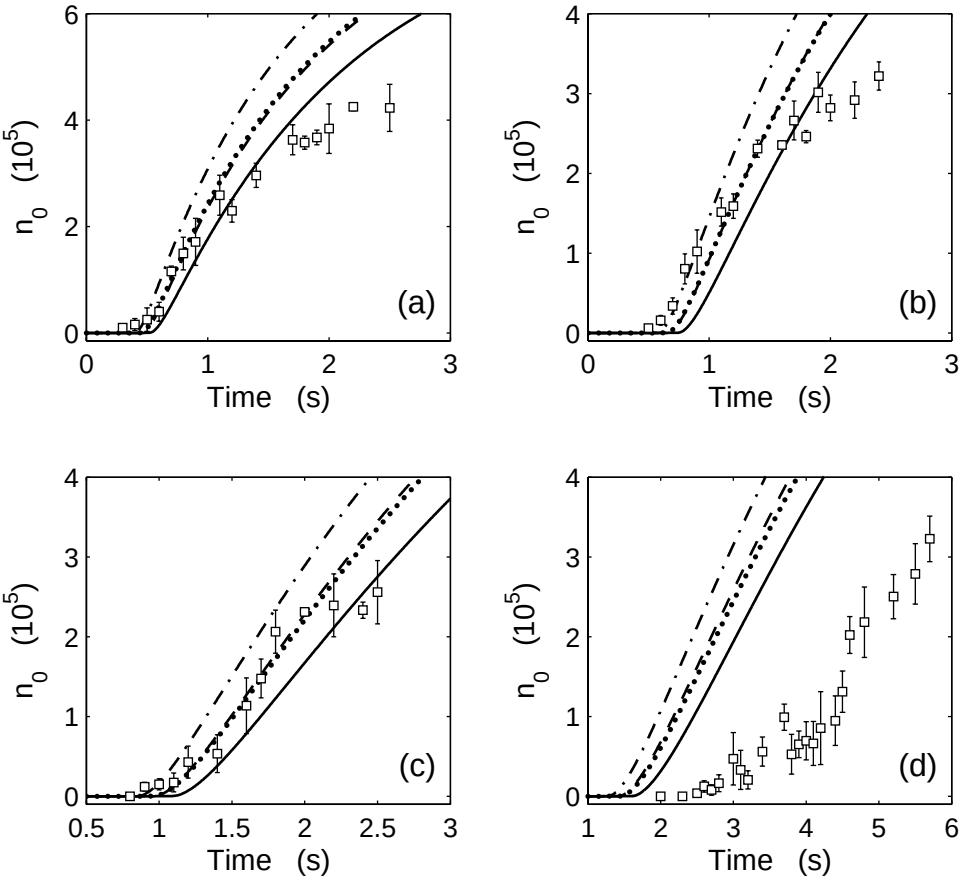

Figure 6. Comparison of theory and experiment for the growth of a ^{87}Rb Bose-Einstein condensate. The squares with error bars indicate the experimental data, while each line is the theoretical prediction based on a slightly different initial condition. Each graph is for a different rf frequency ν. Solid: $N_i = 4.2 \times 10^6$, $T_i = 640$ nK, $\mu_{\rm init} = -300\hbar\bar{\omega}$. Dashed: $N_i = 4.4 \times 10^6$, $T_i = 640$ nK, $\mu_{\rm init} = -289\hbar\bar{\omega}$. Dotted: $N_i = 4.2 \times 10^6$, $T_i = 610$ nK, $\mu_{\rm init} = -254\hbar\bar{\omega}$. Dot-dash: $N_i = 4.4 \times 10^6$, $T_i = 610$ nK, $\mu_{\rm init} = -244\hbar\bar{\omega}$. (a) $\nu = 2060$ kHz. (b) $\nu = 2070$ kHz. (c) $\nu = 2080$ kHz. (d) $\nu = 2090$ kHz.

three body loss coefficient K_3 for this experimental set up may be different from that reported in [15]; however, this is difficult to estimate.

The one instance where theory and experiment differ strongly is for the slowest cooling experiment with an rf frequency of 2090 kHz, for which the comparison is plotted in figure 6(d). The experimental data has the peculiar feature that there is an apparent sudden increase in the growth rate just over four seconds after the beginning of the experiment. In [12] it is suggested that this jump is due to strong phase fluctuations in the initial elongated condensate [17]. This feature, also known as quasicondensation, was first suggested as a stage in the growth of a BEC by Kagan *et al* [18]. Recently phase fluctuations have been observed experimentally in elongated condensates [19].

This behaviour can be explained physically as follows. The initially strong phase fluctuations can be thought of as the condensate having been seeded in several parts,

and thus bosonic stimulation occurs for each part separately. Therefore, the initial growth rate will be slower than would otherwise be predicted theoretically. As the phase coherence length grows, however, suddenly a true condensate will form from the parts and there will be a corresponding jump in the growth rate.

The lack of agreement between theory and the experimental data for the rf frequency of 2090 kHz suggests that an effect not included in our model is becoming important. The experimentally observed initiation time is close to that predicted by the theory, however the initial growth rate is much reduced. Our model of condensate growth makes the assumption that only a single condensate forms in the system, and this is represented by a single quantum level. Therefore, the model currently cannot represent slower initial growth due to the presence of any quasicondensate. However, once the "true" condensate forms the observed growth rate does appear to be similar to that predicted by the simulations, but at a later time.

4. Conclusions

We have extended our model of condensate growth [10] to take into account the sag of the atomic trapping potential due to gravity, and the effect this has on evaporative cooling at low temperature. We have described the effect this has on growth experiments, and carried out a comparison with all available experimental data taken by the Munich group and presented in [12]. We have found that despite the many approximations made, the theoretical model is, for the most part, in good agreement with the experimental data. It has been suggested for the one case in which there is a discrepancy that this is due to the effects of quasicondensation—a hypothesis that is not contradicted by our calculations.

Acknowledgments

The authors would like to thank Michael Köhl for many useful discussions and for the provision of the experimental data before publication. This work was supported by the Engineering and Physical Sciences Research Council in the United Kingdom, and by the Royal Society of New Zealand under the Marsden Fund Contract No. PVT-902.

References

[1] Anderson M, Ensher JR, Matthews MR, Wieman CE and Cornell EA 1995 *Science* **269** 198
[2] Davis KB, Mewes M-O, Andrews MR, van Druten NJ, Durfee DS, Kurn DM and Ketterle W 1995 *Phys. Rev. Lett.* **75** 3969
[3] Bradley CC, Sackett CA, Tollet JJ and Hulet R 1995 *Phys. Rev. Lett.* **75** 1687; 1997 *Phys. Rev. Lett.* **79** 1170
[4] Stoof HTC 1999 *J. Low Temp. Phys.* **114** 11
[5] Gardiner CW and Zoller P 1997 *Phys. Rev.* A **55** 2902; Gardiner CW and Zoller P 1998 *Phys. Rev.* A **58** 536; Gardiner CW and Zoller P 2000 *Phys. Rev.* A **61** 033601
[6] Miesner HJ, Stamper-Kurn DM, Andrews MR, Durfee DS, Inouye S and Ketterle W 1998 *Science* **279** 1005

[7] Gardiner CW, Ballagh RJ, Davis MJ and Zoller P 1997 *Phys. Rev. Lett.* **79** 1793
[8] Gardiner CW, Lee MD, Ballagh RJ, Davis MJ and Zoller P 1998 *Phys. Rev. Lett.* **81** 5266
[9] Lee MD and Gardiner CW *Phys. Rev.* A **62** 033606
[10] Davis MJ, Gardiner CW, and Ballagh RJ 2000 *Phys. Rev.* A **62** 063608
[11] Bijlsma MJ, Zaremba E and Stoof HTC 2000 *Phys. Rev.* A **62** 063609
[12] Köhl M, Davis MJ, Gardiner CW, Hänsch T and Esslinger T 2001 *Preprint* cond-mat/0106642
[13] Dalfovo F, Giorgini S, Pitaevskii LP and Stringari S 1999 *Rev. Mod. Phys.* **71** 463
[14] Söding J, Guéry-Odelin D, Desbiolles P, Chevy F, Inamori H and Dalibard J 1999 *Appl. Phys.* B **69** 257
[15] Burt EA, Ghrist RW, Myatt CJ, Holland MJ, Cornell EA and Wieman CE 1997 *Phys. Rev. Lett.* **79** 337
[16] Köhl M 2001, *Private communication*
[17] Petrov DS, Shlyapnikov GV and Walraven JTM 2001 *Preprint* cond-mat/0104373
[18] Kagan Yu, Svistunov BV and Shlyapnikov GV 1992 *Zh. Eksp. Teor. Fiz.* **101** 528 (1992 *Sov. Phys. JETP* **75** 387)
[19] Dettmer S, Hellweg D, Arlt J, Ertmer W, Sengstock K, Petrov DS, Shlyapnikov GV, Kreutzmann H, Santos L and Lewenstein M 2001 *Phys. Rev. Lett.* **87** 160406